

Analysis of Tool-Chip Interface Temperature with FEM and Empirical Verification

M. Bagheri, P. Mottaghizadeh

Abstract—Reliable information about tool temperature distribution is of central importance in metal cutting. In this study, tool-chip interface temperature was determined in cutting of ST37 steel workpiece by applying HSS as the cutting tool in dry turning. Two different approaches were implemented for temperature measuring: an embedded thermocouple (RTD) in to the cutting tool and infrared (IR) camera. Comparisons are made between experimental data and results of MSC.SuperForm and FLUENT software.

An investigation of heat generation in cutting tool was performed by varying cutting parameters at the stable cutting tool geometry and results were saved in a computer; then the diagrams of tool temperature vs. various cutting parameters were obtained. The experimental results reveal that the main factors of the increasing cutting temperature are cutting speed (V), feed rate (S) and depth of cut (h), respectively. It was also determined that simultaneously change in cutting speed and feed rate has the maximum effect on increasing cutting temperature.

Keywords—Cutting parameters, Finite element modeling, Temperature measurement, Tool-chip interface temperature.

I. INTRODUCTION

THE resultant heat of metal cutting is one of the limiting factors of machining processes. This phenomenon has adverse impacts on the manufactured tool, dimensional accuracy, tool wear, speed and cost of production. On the other hand, consumption of cutting fluid used in metal machining for a variety of reasons such as improving tool life, surface finish and flushing away chips from the cutting zone, has become a health detriment to the operator as well as a contaminant into the environment. Hence, abatement and avoidance of using cutting fluids in machining operations have been among vital issues during recent years.

In 1907, Taylor presented his first research article on the role of heat in metal cutting processes. This theory suggested that if the cutting temperature rises, tool-wear increases which leads to damages and thermal stresses in the workpiece [1], [2]. Until 1920s, there has been no discussion about heat in machining and tool temperature in United States, however, Shaw proposed concepts in these areas in 1924 and simultaneously, Gottwin in Germany (1928) and Herrbert in England (1920) carried out experiments with the purpose of temperature measurement along the cutting tool surface in tool-workpiece turning using the thermocouple technique [3].

M. Bagheri is a graduate student of mechanical engineering, Amirkabir University of Technology (Tehran Polytechnic), Tehran, Iran (phone: +98-912-240-9815; e-mail: m.bagheri.mech@gmail.com).

P. Mottaghizadeh is graduated of chemical engineering, Amirkabir University of Technology (Tehran Polytechnic), Tehran, Iran (e-mail: p.mottaghizadeh@gmail.com).

In 1983, Stephenson, by using the results of the high strain rate torsion tests under adiabatic circumstances and based on strain rate variables acquired flow stress and heat [2]. In 1990, Moraka examined effects of rake angle and various cutting parameters on the temperature distribution along the rake face by applying finite element method. Heat generation rate is evaluated by means of some experimental methods that determine the value of strain in primary and secondary deformation zones [3]. The effect of friction on orthogonal cutting operation was studied by Shay and et al. in 2003 using finite element method, in which the orthogonal cutting process was modeled under plane strain condition [4].

II. HEAT IN CUTTING PROCESS

Empirical temperature distribution in workpiece and chip during cutting process is shown in Fig. 1 [5]. Point X of workpiece moves toward tool and reaches to the primary deformation zone; then its temperature rises till it abandons this zone as a chip. Whereas point Y passes through both of deformation zones and warms up until it leaves the secondary deformation zone. Once it passes this zone, some of its heat conveys to chip via conduction and finally all parts of the chip gets homogeneous temperature. Thus, the maximum temperature of a spot on rake face of tool is very close to its cutting edge. Point Z, which stays on workpiece, warms through conduction of primary deformation zone.

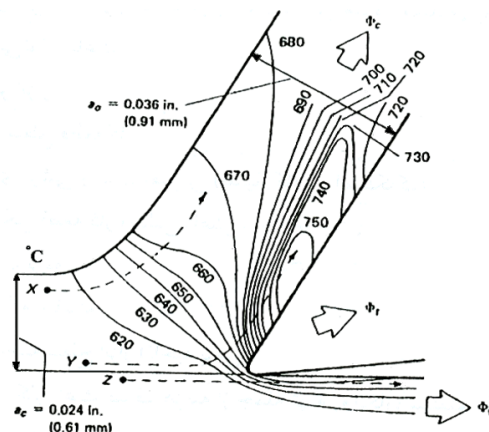


Fig. 1 Temperature distribution in chip and workpiece during cutting process [9]

Furthermore, some amount of heat enters tool from secondary deformation zone [5]; therefore, the following equation can be written.

$$P_m = \Phi_c + \Phi_w + \Phi_t \quad (1)$$

In (1), P_m is total rate of heat generation, Φ_c is rate of heat transfer by chip, Φ_w is rate of heat conduction to workpiece and Φ_t is rate of heat conduction to tool.

Due to high velocity of workpiece movement on tool rake face, heat transfer through chip is considerably more than that of through tool. Consequently, Φ_t constitutes insignificant amount of P_m and could be neglected unless the cutting speed is very low.

III. HEAT TRANSFER MODELING OF TOOL

Thermal modeling of cutting processes consists of two stages:

- 1) Chip formation process and its temperature,
- 2) Heat transfer analysis of tool.

Modeling of chip formation process is performed by MSC.SuperForm software, while heat transfer analysis of tool is accomplished through FLUENT software due to the fact that MSC.SuperForm cannot display the temperature distribution of various points under the tool, where thermocouple is installed. In addition, the time of chip formation analysis is not enough to this task.

A. Modeling of chip formation process by MSC.SuperForm

In this paper, like any other studies, there have been some simplifying assumptions in order to simulating the process; these assumptions are:

- 1) Orthogonal machining process is assumed in steady- state conditions,
- 2) Tool is presumed as a rigid body,
- 3) Chip shape is assumed to be continuous,
- 4) Workpiece is assumed to be Elastic-Viscoplastic [7].

These simplifying assumptions, which are applied either explicitly or implicitly to obtain models, inevitably may cause some errors. These errors are discovered in comparison between experimental results and simulation data [7].

Variable cutting parameters are cutting speed, feed rate, depth of cut, and radius of main cutting edge of tool. In this model, the applied tool is assumed rigid body and the workpiece material is equivalent to structural steel whose characteristics could be found in software database. Behavior of the workpiece is assumed as Elastic-Viscoplastic and is modeled based on changes of its properties due to temperature. In this study, separation criterion of chip is based on critical stress at the tip of the tool. The shear stress was investigated at each incremental move tool and when this stress was more than specified criterion, element leaves the front tip of the tool in shape of chip. In this model, chip shape is assumed to be continuous. Columbus friction law is used in modeling of friction and two friction zones of adhesion and sliding are considered on the rake face of machining tool. Sliding friction coefficient is assumed of 0.5. In all made models, the whole finite element parameters are set on constant values, for instance, the number of elements and nodes, type of elements, and size of elements have stable values.

However, machining parameters individually varies in each simulation. In simulations where one parameter is changing, others must be fixed so that accurate results will show the effect of that certain parameter.

In this work, many various simulations for a tool with sharp with sharp edge (the main cutting edge radius is zero) were prepared that include simulations for variable cutting speed and variable feed rate. In addition, many simulations were organized for cutting edge radius of 0.025, 0.05, 0.1 mm (while other parameters were considered fixed). In some of the simulations, depth of cut was changed. Most these simulations were made equivalent to empirical situations.

In this simulation, workpiece is a rectangular with dimensions of 6.3 mm in 3.1 mm, in which the length and the width is divided into 40 and 10 equal parts, respectively. The number of elements before remeshing was the constant amount of 400 (equivalent to 451 nodes). The rake angle and relief angle are assumed 2 and 4 degree, respectively, which is fixed during all simulation states. Initial temperature of tool and workpiece is considered the constant amount of 20°C.

With respect to the boundary conditions used in these simulations, solid curves are considered as the tool wall. Nodes that are fixed on the wall do not have any displacement or rotation in any direction. Last right nodes of workpiece are kept constant with a rigid wall, and bottom nodes are kept at constant depth by a symmetry line. These nodes do not have any displacement neither in direction of cutting speed nor feed rate during the cutting operation. Tool, which is considered as a rigid body, moves from left to right at constant speed in a straight line. After the contact of tool with workpiece (elements), once the first node's stress reaches to its critical value, this node is separated from the rest of elements and is transmitted to chip-tool interface, then leaves the workpiece as a chip. Fig. 2 shows a two-dimensional model of orthogonal cutting process by finite element modeling; thus, the parameters of cutting speed, depth of cut, feed rate and cutting edge radius change as the variables in the software.

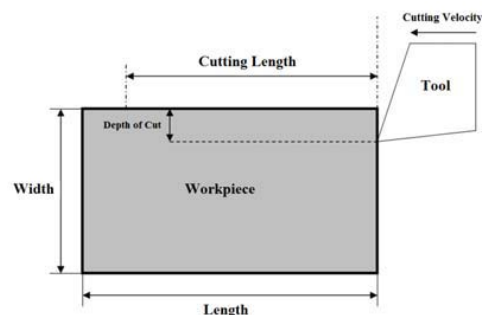


Fig. 2 Orthogonal cutting model in finite element modeling

In this paper, flow stress of workpiece material is function of strain, strain rate and temperature (with considering the effect of large strain, strain rate and temperature of cutting properties associated with the work piece). Cutting process from the beginning to steady state was simulated by the help of step by step cutting tool's movement.

In this model, the chip separation criterion was assumed based on a critical distance from the edge of tool, which was performed by applying mark code through subprogram of adaptive remeshing in software. Chip shape, temperature fields, stress distribution, strain and strain rate in chip, were all determined in chip, workpiece and tool. Parameters of adaptive remeshing pertinent to the modeling of the chip formation are shown in Table I. It should be noted that these parameters are constant in the whole process and through trial and error method they are selected as the best parameters.

Finite element model in MSC.SuperForm, the way of chip formation and temperature field in tool are shown in Fig. 3.

TABLE I
CHARACTERISTICS OF REMESHING PARAMETERS

Remeshing Parameter	Description
Remeshing method	Progressive square mesh
Displacement frequency	1
Length of element edge	0.11625 mm
Corner angle	120 degree
Dividing curve control	36
Smoothing ratio	0.5

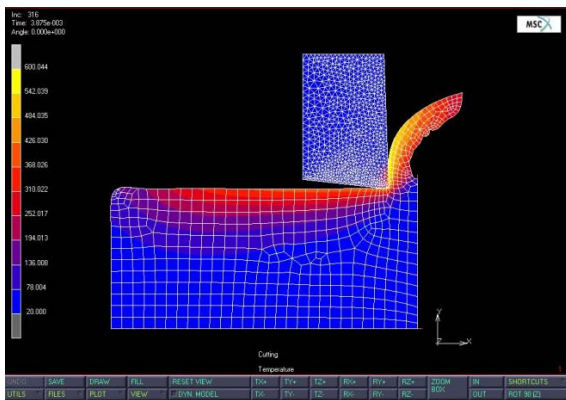


Fig. 3 chip formation process and temperature distribution in H.S.S tool with rake angle of in MSC.SuperForm.

A. Modeling of chip formation process by FLUENT

Nodal temperatures of tool-chip interface as well as heat flux in these nodes, which are obtained from SuperForm, were considered as initial conditions for heat transfer analysis in FLUENT. Analysis time of approaching to experimental conditions is assumed 60 seconds as after 30 seconds temperature distribution in tool became stabilized.

In order to compare simulated temperature by software with measured temperature by infrared camera (IR), chip formation results can be used. However, in case the thermocouple located at 0.5 mm distance from tool rake face, heat transfer analysis results of FLUENT should be used since chip formation time for heat transfer to the whole tool is very short. Fig. 4 displays the temperature distribution in HSS tool after heat transfer analysis.

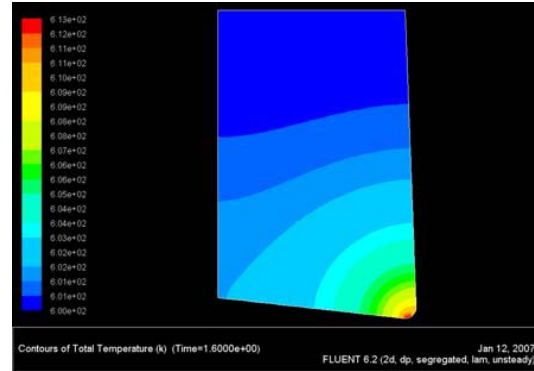


Fig. 4 Temperature distribution in heat transfer analysis by FLUENT for HSS tool with rake angle of 2°

IV. EXPERIMENTAL TESTS

In this study, two methods of tool temperature evaluation are presented:

- 1) The placement of thermocouple in the tool
- 2) The infrared thermometer

In the following, first the set of instruments and experiments are explained and then each of the methods will be demonstrated.

A. Experiment Sample

The experimental conditions were identical in both methods, and process is performed by H.S.S cutting tool with fixed geometry (2° rake angle) on a 100 mm diameter tubular workpiece of structural steel.

B. Thermocouple

According to standard tables of the thermocouples and considering available sensors on the market, thin-film-platinum type of RTD resistive sensor (PT-RTD) has been used; and in order to achieve minimum error rate and high response time, a sensor with low ohm model (PT-100) was used. The advantages of this sensor are its linear system, high thermal range, great accuracy, repeatability.

Heat measurement in PT-RTD is based on determination of electric resistance. Resistance changes are linearly dependent on temperature variations; this relation could be defined by a mathematical and experimental model in detail as follows

$$RT = R_0 [1 + aT - bT^2 - cT^3(T - 100)] \quad (2)$$

In (2), RT is the resistance at a certain temperature T , R_0 is the resistance at 0°C and a , b , c are constants of (2) whose values are demonstrated in Table II.

C. RTD Sensor Accessories

With respect to the type of selected sensor, PT-100, it is necessary to design a system in which sensor resistance value changes can properly convert to readable thermal values that could be registered. For this purpose, an Analog-to-Digital converter board (A/D board) was designed, fabricated and

located in the sensor so that it could read the analog resistance values and convert them to digital values.

TABLE II
VALUES OF COEFFICIENTS OF THE CHARACTERISTIC EQUATION FOR RTD
RESISTANCE

Tempature	a	b	c
$T < 0\text{ }^{\circ}\text{C}$	3.90802×10^{-3}	5.80195×10^{-7}	4.27351×10^{-12}
$T = 0\text{ }^{\circ}\text{C}$	3.90802×10^{-3}	5.80195×10^{-7}	0

Also, in order to accomplish the experiments, it is required to embed the respective sensor in desired position of sensor and then connect the tool and sensor set to a pen turning lathe. In addition to the convenience application of tool to examine any machining parameter, sensor is reliably placed in tool and is connected to the A/D board and then to computer through an extension cord. To achieve this objective, a tool holder was designed and assembled; exploded view of holder and assembled parts are shown in Fig. 5.

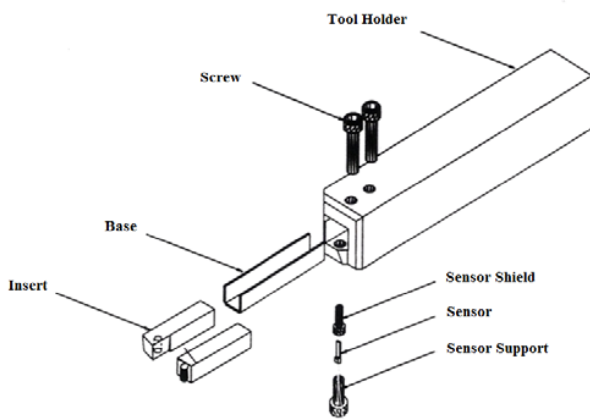


Fig. 5 Exploded view of tool and tool holder with sensor accessories

D. Infrared Camera (IR)

Many studies have been made on emitted infrared radiation technique for temperature measurement. This technique has numerous advantages over other techniques due to the fact that most of materials used in cutting tools like ceramics, which are used in high speed machining, have some physical properties such as brittleness and high electrical resistance that may harm during turning process; hence, it is difficult to use contact sensors like thermocouples which are placed on tool to evaluate the very exact temperature of tool- chip joint. This method is actually a non-contact technique for measuring body temperature based on heat energy of emitted radiation from objects [8]. A type of an infrared camera device use for surface temperature measurement in this study is shown in Fig. 6.



Fig. 6 Infrared camera

Some this infrared camera features are given in Table III.

E. K-Type Thermocouple Display

In order to display the temperature of K-Type Rod

TABLE III
SPECIFICATIONS OF INFRARED CAMERA

Characteristic	Description
Measurable Temperature range	-3 to 900 °C
Resolution	0.1 °C
Accuracy of data at 25°C	±0.75% of read value
Repeatability	±0.5% of read value
Response Time (±0.95%)	250 mSec
Hot Spot Detection (30%)	85 mSec
Wave amplitude	8-14µm
Allowable temperature in the workplace	0-50 °C
Analogue output	1 mV/°C
Digital output	USB 1.1
Effective flash range	0.5-2 m
Light sensitivity	6 lux

Thermocouple, TESTO 922 thermometer, which has two temperature inputs, was used. This thermocouple is used for comparison and camera calibration. The display is shown in Fig. 7.



Fig. 7 K-Type thermocouple display

F. Assembly and System Preparation for Test

To situate the camera on the lathe for recording temperatures, it was necessary to have a mechanism in which camera could be kept constant so as to remain safe against hand vibration and other quiver errors. For this purpose, a clock base was used as a stand camera, and then camera was attached to that stand a bush design. The advantage of this is that the stand is adjustable in all directions. Furthermore, this is a magnetic stand which could be installed anywhere in the system as necessary. Thus, camera could be located in the best position to record the tool temperature by trial and error method which is depicted in Fig. 8.

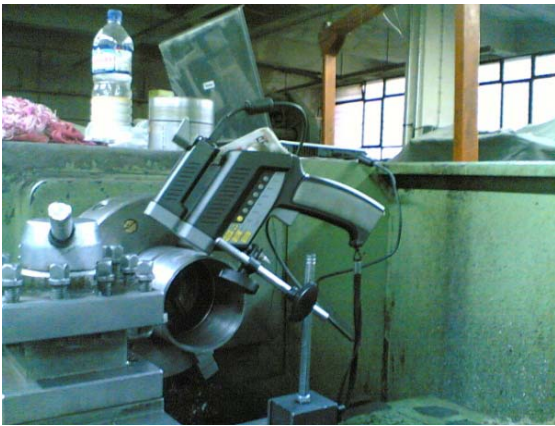


Fig. 8 Infrared camera installation on the lathe

In order to ensure proper performance of the camera, the resulted data were compared with those of K-type rod thermocouple; also, camera resolution was determined by running experiment for 5 times at various cutting speed. In this test, camera sheds infrared light on a point near the cutting spot of the tool, exactly where a rod thermocouple is installed; hence, the results of these two methods could be simultaneously.

All materials emit radiant energy; the extent to which a material emits thermal energy depends on its temperature. Emittted energy can be estimated by the Stefan-Boltzmann law as follows

$$q_e = \varepsilon \cdot \sigma \cdot T^4 \quad (2)$$

In (3), ε is emission coefficient of the object, σ is Stefan-Boltzmann's constant ($5.675 \times 10^{-8} (W.m^{-2}.K^{-4})$) and T is the object's temperature.

In this camera, parameter ε , which varies for different materials, is adjustable. For polished objects this coefficient reaches 0.1, while for uncoated carbide tools $\varepsilon = 0.3$ [11]. In this set of experiments, this coefficient is considered as $\varepsilon = 0.23$ for HSS cutting tool and the distance of camera from cutting zone is about 120 mm, which is considered the optimum distance. This conclusion was achieved based on

comparison of temperature data between measurement techniques of IR camera at various ε and the rod thermocouple. Then, according to the given explanations, measuring equipments were assembled. It is worth noting that based on IR camera's data we used a laptop on which camera software was installed so that data reading could be performed on-line. It is also noteworthy to mention that presence of shear rate and high temperature gradient has made the response time an important criterion in temperature measurement; this is an advantage of IR camera in comparison with thermocouple which has a relatively longer response time.

V. ANALYSIS OF EXPERIMENTAL RESULTS

A. Study of Cutting Speed Effect on Cutting Tool Temperature

This experiment was conducted in workshop conditions and only by changing rotation axis and the diameter of the workpiece, different values of cutting speed (V) were obtained while other cutting parameters were stable. Results derived from the thermocouple and IR camera measurements are presented in Fig. 9 and Fig. 10, respectively. Vertical axis corresponds to the measured temperature within the tool. It can be observed that in the beginning of experiment, temperature values ascend with a relatively steep slope and as time passes, the curve slope decreases and reaches approximately zero.

TABLE IV
TEST CONDITIONS FOR ANALYSIS OF CUTTING SPEED EFFECT

Characteristic	Description
Tool characteristics	HSS
Rake angle	2°
Free angle	4°
Workpiece specification	ST37 steel
Cutting speed (variable)	131, 185, 263, 528, 733 mm/s
Feed rate	0.08 mm/rev
Depth of cut	1.5 mm

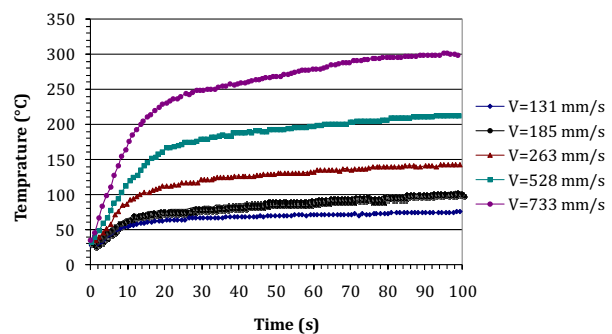


Fig. 9 HSS cutting tool temperature at various levels of cutting speed (RTD)

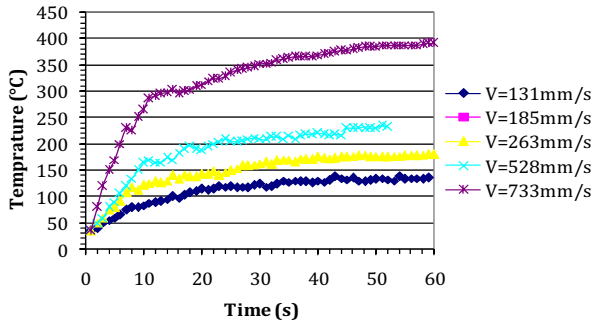


Fig. 10 HSS cutting tool temperature at various levels of cutting speed (IR camera)

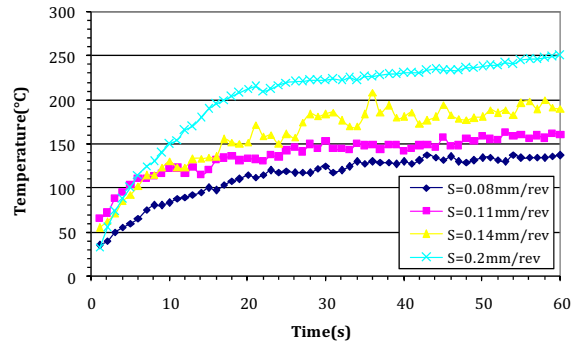


Fig. 12 HSS cutting tool temperature at various levels of feed rate (IR camera)

B. Study of Feed Rate Effect on Cutting Tool Temperature

In these experiments, with changes in feed rates (S), resulted values of temperature within the pen were recorded by means of computer. Cutting parameters and tool angles and another condition of these researches are given in the Table V. The results of the tests by the IR camera and thermocouple are shown in Fig. 11 and Fig. 12.

TABLE V
TEST CONDITION FOR ANALYSIS OF FEED RATE EFFECT

Characteristic	Description
Tool characteristics	HSS
Rake angle	2°
Free angle	4°
Workpiece specification	ST37 steel
Cutting speed	131 mm/s
Feed rate (variable)	0.08, 0.11, 0.14, 0.2 mm/rev
Depth of cut	1.5 mm

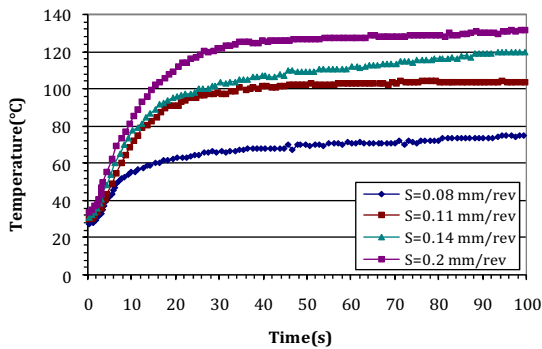


Fig. 11 HSS cutting tool temperature at various levels of feed rate (RTD)

C. Study of Depth of Cut Effect on Cutting Tool Temperature

In the third experiment, by keeping all cutting parameters constant and changing the depth of cut factor, effects of this varying parameter was examined. Experimental conditions for this run are presented in Table VI. The results of these tests by the IR camera and thermocouple are presented in Fig. 11 and

TABLE VI
TEST CONDITION FOR ANALYSIS OF DEPTH OF CUT EFFECT

Characteristic	Description
Tool characteristics	HSS
Rake angle	2°
Free angle	4°
Workpiece specification	ST37 steel
Cutting speed	131 mm/s
Feed rate (variable)	0.08 mm/rev
Depth of cut	1.5, 2.1, 2.94, 4.1 mm

Fig. 12, respectively.

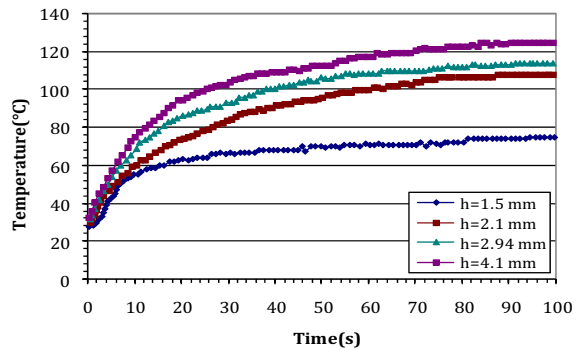


Fig. 13 HSS cutting tool temperature at various levels of depth of cut (RTD)

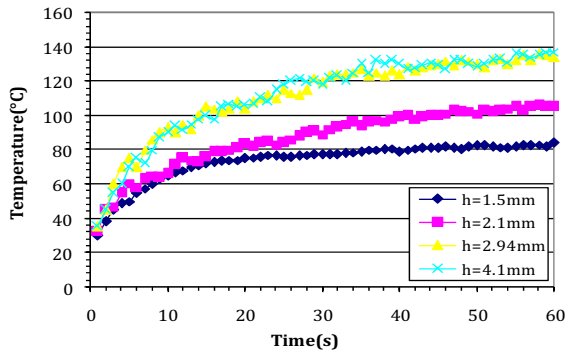


Fig. 14 HSS cutting tool temperature at various levels of depth of cut (IR camera)

An important point of this test (third experiment) is that the final temperature or equilibrium temperature is less than that of previous test; also, temperature gradient is much more less than other tests which means that depth of cut is a less significant parameter in heat generation compared with other parameters during the cutting operation.

VI. STUDY OF HEAT GENERATION FACTORS ON CUTTING TOOL THROUGH EXPERIMENTAL DESIGN TECHNIQUE

It is assumed that the only effective factors in heat generation of cutting tool are three parameters of cutting speed, feed rate and depth of cut. Here, the three machining parameters or three factors as well as two levels are considered. However, in practice, number of factors may be more and also applied levels can be more than assumption during use of experimental design. According to a number of factors (three factors) and considered number of levels (two levels), a full-factorial design was employed in this study. It should be noted that for N-factor in two levels, 2^N design is applied. Consequently, in this example we have 32 models (or eight components) to test [9]. Full-factorial design matrix with three factors and two levels along with their main effects and interactions of factors are in accordance with the Table VIII. It should be noticed that negative sign denotes the lower levels or less values of each factor; nevertheless, positive sign indicates either upper levels or more amounts of each factor. It is worth mentioning that each of the second level factors has had about 40 percent growth regarding the first level factors.

TABLE VII
TEST CONDITION FOR ANALYSIS OF DEPTH OF CUT EFFECT

Parameters	First level (-)	Second level (+)
Cutting speed (A)	7.9 m/min	11.1 m/min
Feed rate (B)	0.08 mm/rev	0.11 mm/rev
Depth of cut (C)	1.5 mm	2.1 mm

TABLE VIII
FULL-FACTORIAL DESIGN MATRIX FOR THREE FACTORS

Run No.	A	B	AB	C	AC	BC	ABC
1	-	-	+	-	+	+	-
2	-	-	+	+	-	-	+
3	-	+	-	-	+	-	+
4	-	+	-	+	-	+	-
5	+	-	-	-	-	+	+
6	+	-	-	+	+	-	-
7	+	+	+	-	-	-	-
8	+	+	+	+	+	+	+

It should be considered that in order to ensure the accuracy of the obtained data, it is necessary to reiterate the test at least for 5 times to analyze three factors in each case; however, due to limited facilities in these experiments, only three replications were performed for each mode, which will increase the percent error in the results. Values of each effective factor are presented in Table X.

Obviously from Fig. 15, it could be recognized that the most effectual factor in heat generation is cutting speed, and after that, feed rate and depth of cut and interaction of the three factors have the most effect on heat generation, respectively. The notable point is that the effective value of feed rate is approximately close to that of cutting speed which needs more contemplation. To study this issue and analyze results more strenuous, these two parameters were examined at two other levels whose results are shown in Table XI. Bar chart of each effective value is given in Fig. 16.

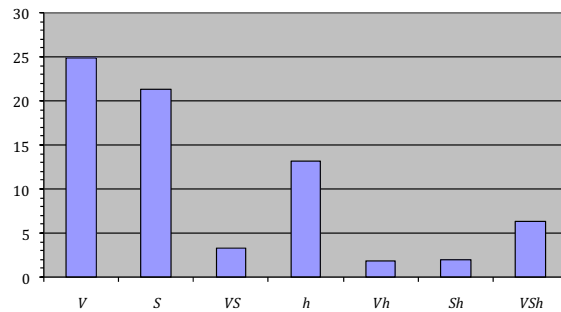


Fig. 15 Bar chart of effective values of each factor in the heat generation within cutting tool

TABLE XI
LEVELS AND VALUES OF EACH FACTOR

Parameters	First level (-)	Second level (+)
Cutting speed (A)	11.1 m/min	15.8 m/min
Feed rate (B)	0.11 mm/rev	0.14 mm/rev
Depth of cut (C)	2.1 mm	2.94 mm

TABLE IX
FULL-FACTORIAL MATRIX FOR ANALYSIS OF HEAT GENERATION IN CUTTING TOOL

Run No.	<i>V</i>	<i>S</i>	<i>V.S</i>	<i>h</i>	<i>V.h</i>	<i>S.h</i>	<i>V.S.h</i>	<i>T</i> ₁	<i>T</i> ₂	<i>T</i> ₃
1	-	-	+	-	+	+	-	74	78	71
2	-	-	+	+	-	-	+	91	84	95
3	-	+	-	-	+	-	+	95	92	103
4	-	+	-	+	-	+	-	102	103	106
5	+	-	-	-	-	+	+	97	104	100
6	+	-	-	+	+	-	-	109	103	109
7	+	+	+	-	-	-	-	117	113	120
8	+	+	+	+	+	+	+	136	143	141

TABLE X
CALCULATION OF VALUES OF EACH CUTTING PARAMETERS EFFECTS IN HEAT GENERATION

Parameter	<i>V</i>	<i>S</i>	<i>V.S</i>	<i>h</i>	<i>V.h</i>	<i>S.h</i>	<i>V.S.h</i>
Average							
<i>T</i> _{avg} (-)	155.25	175.42	188.5	184.17	188.92	189.1	189.67
<i>T</i> _{avg} (+)	225	204.83	191.75	196.1	191.33	191.17	190.58
Δ	69.75	29.41	3.25	11.93	2.41	2.07	0.91

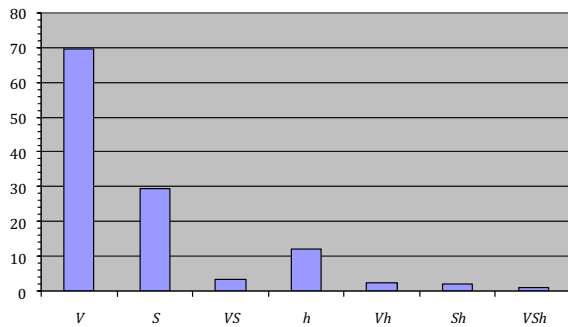


Fig. 16 Bar chart of effective values of each factor in the heat generation within the cutting tool

According to the acquired results and the comparison between them and previous experimental data, it is clarified that cutting speed factor has much more influence on heat generation cutting tool and a huge gap has generates between this factor and other parameters, which denotes the significance of cutting speed parameter in heat generation within the tool, particularly in high cutting speed. This conclusion actually confirms Taylor theory about cutting speed impact on tool wear, which considers cutting speed factor as a crucial determining parameter in tool life.

Based on the results of these experiments, equation of temperature estimation in cutting tool is as following.

$$T = \bar{T} + \left(\frac{\Delta V}{2}\right)V + \left(\frac{\Delta S}{2}\right)S + \left(\frac{\Delta h}{2}\right)h + \left(\frac{\Delta VS}{2}\right)VS \quad (4)$$

Since the effects of interactions of *V.h*, *S.h* and *V.S.h* are very low, their effect is neglected to simplify the equation. In this equation, *T* is the predicted temperature and \bar{T} is

average of all acquired temperatures in these experiments and $\frac{\Delta}{2}$ is half effect value for each of the parameters. Hence, the temperature estimation (4) could be written in the following form

$$T = 10358 + (1242)V + (10.665)S + (6.585)h + (3.165)VS \quad (5)$$

Now, by means of this equation we can maintain the temperature in a specific range mostly in dry machining; by putting a specified temperature in one side of the equation and choosing two levels for parameters of *V* and *S*, the last parameter (depth of cut *h*) is achieved. It should be noted that parameter values are in form of code values (+1 or -1) and the obtained value for the unknown parameter is in code form that must be converted to real value.

VII. RESULTS AND DISCUSSIONS

In this paper, two techniques of temperature measurement, thermocouple placement in the tool and infrared camera was used to estimate the cutting temperature; then the results were compared with finite element analysis through FLUENT and MSC.SuperForm software. According to Fig. 17, results exhibit the effect of cutting speed on tool temperature; in addition, it compares experimental diagrams with finite element analysis results. Fig. 18 shows the effect of feed rate increase on cutting tool temperature; it can be observed that slope of experimental diagram for feed rate is less than that of cutting speed. Fig. 19 shows the temperature variation with depth of cut and it can be observed that with increase of depth of cut, slope of diagram declines and in high levels of depth of cut this slope tends toward zero. Slope of this curve is less than that of cutting speed and feed rate which reveals the fact

that depth of cut is less effective than other parameters. Therefore, the easiest cutting parameter to adjust is the depth of cut; feed rate is the second most likely parameter to increase to gain added productivity.

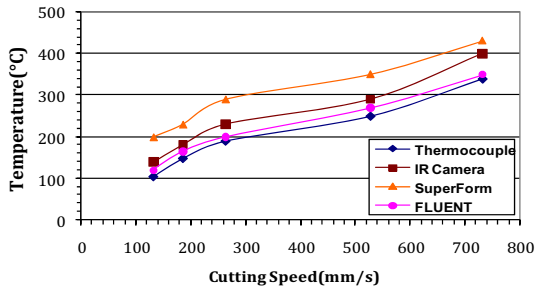


Fig. 17 Diagram of temperature vs. cutting speed

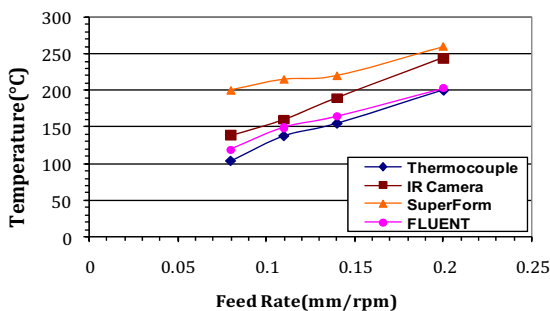


Fig. 18 Diagram of temperature vs. feed rate

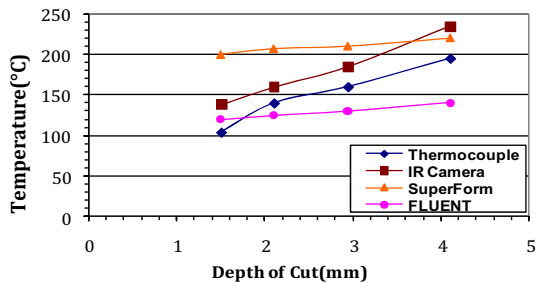


Fig. 19 Diagram of temperature vs. depth of cut

By increasing the cutting speed, temperature rises dramatically; while diagram of temperature vs. feed rate has a less slope. Depth of cut also influences on temperature, however it is less effective than two previously mentioned parameters; as you can see in Fig. 19 the slope of temperature vs. depth of cut is less than others. In a particular range, with further increase in depth of cut, based on material of tool and workpiece, temperature curve in cutting zone becomes almost a straight line with slight slope. Thus, in high levels of depth of cut, cutting zone heat is not affected remarkably by depth of cut rises. Hence, in order to increase machining efficiency, first depth of cut is maximized and then other cutting parameters are considered.

VIII. CONCLUSION

Chip removal process (cutting) is a very sophisticated and unpredictable process; thus, estimation of temperature distribution at the tool-chip interface is a demanding task. In this paper, HSS tool temperature is estimated during machining of ST37 steel through two temperature techniques including thermocouple placement in tool (RTD) and infrared camera (IR). Also, experimental data were compared with results of FLUENT and MSC.SuperForm software. The purpose of this is to establish a correlation between cutting temperature (tool temperature) and main parameters of machining including cutting speed, feed rate and depth of cut.

According to the experiments the following results were obtained:

- 1) Temperature measured by RTD is in a good compliance with FLUENT software results at a point with a distance of 0.5mm from surface of the tool; in this software, after a period of 30 seconds, the temperature distribution in the tool reaches an almost constant value which is in consistent with diagrams of the experimental temperature.
- 2) Measured temperature on surface of tool by means of an infrared camera, reveals more gradient in comparison with MSC.SuperForm software; this is because the spot, where temperature is evaluated through an IR camera, is outside of the tool-chip interface zone while MSC.SuperForm software exactly displays the tool-chip temperature which is more than the measured temperature by IR camera.
- 3) By increasing the cutting speed, tool temperature intensely rises. Cutting speed has a nonlinear relationship with generated heat within tool. Increase of feed rate also raises the tool temperature, however, its effectiveness is less than cutting speed efficacy since temperature diagram of feed rate has a less slope with regard to cutting speed; and in high levels of feed rate, about 0.5 mm/rev to 1 mm/rev, temperature rise has a very slow growth and temperature becomes close to a straight line.
- 4) Temperature will rise by increasing the depth of cut; nevertheless, its impact is less than two other parameters as cutting speed and feed rate. With further increase of depth of cut from a particular range, Depending on the tool and workpiece material, temperature of cutting zone approximates to an almost straight line with low slope. Therefore, in high levels of cutting depth, it is not an effective factor in heat generation within tool. Due to the mentioned fact, in order to enhance efficiency of machining process, it is advisable to increase the cutting depth first and then other cutting parameters are considered.
- 5) By using the experimental results of thermocouple, temperature estimation equation was presented; which reveals that increase of cutting speed, feed rate, cutting depth and interaction between cutting speed and feed rate have the most effect on temperature on tool surface.

REFERENCES

- [1] Milton C.Shaw, "Metal cutting principles," Oxford University Press, Arizona State University, 1984.

- [2] L. Filicie, D. Umbrello "On the finite element codes capability for tool temperature calculation in machining processes," Journal of material processing Technology (2006) 182-190
- [3] H A review of the experimental techniques for the measurement of heat and temperature generated in some manufacturing processes and tribology,(2004) 653-682.
- [4] Boothroyd G.Fundamental metal machining and machine tools. New York McGraw-Hill;1981. p.92-102.
- [5] Ihsan Korkut, Mehmet Boy, Ismail Karacan, Ulvi Seker "Investigation of chip-back temperature during machining depending on cutting parameters" Journal materials & design.
- [6] Larry Barrentine, "Design of experiment," 1999.
- [7] Estimation of Two-dimension Tool Wear Based On Finite Element Method".Hrsg: Prof. Dr.Ing.Jurgen Fleischer & Prof. Dr.Ing. Hartmut Weule. University of Karlsruhe (TH).
- [8] D.O Sullivan, M.Cotterell "Temperature measurement in single point turning" Journal of Material processing & Technology (2001)301-308.
- [9] A. Fata, M.R. Razfar, "Measurement Tool Temperature by Finite Elements Methods," 15th Annual International Iranian Mechanical Engineering Conference, 2007.